Biochem. J. (1975) **152**, 547–559
Printed in Great Britain

Proton Translocation and the Respiratory Nitrate Reductase of *Escherichia coli*

By PETER B. GARLAND, J. ALLAN DOWNIE* and BRUCE A. HADDOCK
Department of Biochemistry, Medical Sciences Institute, University of Dundee, Dundee DD1 4HN, U.K.

(*Received* 26 *June* 1975)

Stoicheiometries and rates of proton translocation associated with respiratory reduction of NO_3^- have been measured for spheroplasts of *Escherichia coli* grown anaerobically in the presence of NO_3^-. Observed stoicheiometries [$\rightarrow H^+/NO_3^-$ ratio; P. Mitchell (1966) *Chemiosmotic Coupling in Oxidative and Photosynthetic Phosphorylation*, Glynn Research, Bodmin] were approx. 4 for L-malate oxidation and approx. 2 for succinate, D-lactate and glycerol oxidation. Measurements of the $\rightarrow H^+/2e^-$ ratio with formate as the reductant and oxygen or NO_3^- as the oxidant were complicated by pH changes associated with formate uptake and CO_2 formation. Nevertheless, it was possible to conclude that the site of formate oxidation is on the inner aspect of the cytoplasmic membrane, that the $\rightarrow H^+/O$ ratio for formate oxidation is approx. 4, and that the $\rightarrow H^+/NO_3^-$ ratio is greater than 2. Measurements of the rate of NO_3^- penetration into osmotically sensitive spheroplasts demonstrated an electrogenic entry of NO_3^- anion. The permeability coefficient for nitrate entry at 30°C was between 10^{-9} and 10^{-10} cm·s^{-1}. The calculated rate of nitrate entry at the concentrations typically used for the assay of nitrate reductase (EC 1.7.99.4) activity was about 0.1% of that required to support the observed rate of nitrate reduction by reduced Benzyl Viologen. Measurements of the distribution of nitrate between the intracellular and extracellular spaces of a haem-less mutant, de-repressed for nitrate reductase but unable to reduce nitrate by the respiratory chain, showed that, irrespective of the presence or the absence of added glucose, nitrate was not concentrated intracellularly. Osmotic-swelling experiments showed that the rate of diffusion of azide anion across the cytoplasmic membrane is relatively low in comparison with the fast diffusion of hydrazoic acid. The inhibitory effect of azide on nitrate reductase was not altered by treatments that modify pH gradients across the cytoplasmic membrane. It is concluded that the nitrate-reducing azide-sensitive site of nitrate reductase is located on the outer aspect of the cytoplasmic membrane. The consequences of this location for mechanisms of proton translocation driven by nitrate reduction are discussed, and lead to the proposal that the nitrate reductase of the cytoplasmic membrane is vectorial, reducing nitrate on the outer aspect of the membrane with $2H^+$ and $2e^-$ that have crossed from the inner aspect of the membrane.

Although the phenomenon of respiration-driven proton translocation (Mitchell, 1966) across the inner mitochondrial membrane (Mitchell & Moyle, 1967) and the cytoplasmic membrane of many bacteria (Scholes & Mitchell, 1970; Jeacocke *et al.*, 1972; West & Mitchell, 1972; Lawford & Haddock, 1973; Meyer & Jones, 1973; Drozd & Jones, 1974; Beatrice & Chappell, 1974; Jones *et al.*, 1975) is well established experimentally, the underlying mechanism is undetermined. A general mechanism proposed by Mitchell (1966) requires that the respiratory chain be arranged as a series of alternating hydrogen and electron carriers so positioned in the membrane to form loops that proton translocation is an inevitable consequence of the transfer of reducing equivalents from substrates to the terminal acceptor, which is usually oxygen. However, a transmembrane arrangement has so far been shown only for the electron-carrying sequence from cytochrome *c* by way of cytochrome $a+a_3$ to oxygen (Hinkle & Mitchell, 1970).

In this present paper we describe stoicheiometries and rates of proton translocation associated with respiratory nitrate reduction by *Escherichia coli*. We describe experiments on the access of nitrate, and its competitive inhibitor azide, to nitrate reductase (EC 1.7.99.4) in whole cells and spheroplasts. The results indicate that the azide-sensitive nitrate-reducing site of nitrate reductase is on the outer aspect of the cytoplasmic membrane. We have already shown

* Present address: Department of Biochemistry, John Curtin School of Medical Research, Australian National University, Canberra City, A.C.T. 2601, Australia.

that $FMNH_2$, a non-physiological reductant in the present context, reacts with nitrate reductase at the inner aspect of the cytoplasmic membrane (Kemp *et al.*, 1975). These findings together show that nitrate reductase spans the membrane, and can catalyse a vectorial reduction of NO_3^- on the outer aspect of the cytoplasmic membrane with reducing equivalents from the inner.

Materials and Methods

Organism

E. coli EMG-2 (K12 Y*mel* prototroph) was kindly provided by Mr. M. Peacey (Department of Molecular Biology, University of Edinburgh, Edinburgh, U.K.) and was used for all experiments except where the intracellular concentration of nitrate was determined, in which case *E. coli* A1004a (Haddock, 1973) was used. Strain A1004a was generously given by Dr. H. U. Schairer (Max-Planck-Institut für Biologie, 73-Tubingen, W. Germany). Stock cultures of bacteria were kept as 4ml suspensions in 15% (v/v) glycerol at −22°C.

Anaerobic growth of bacteria

A preliminary overnight culture of *E. coli* EMG-2 was made by inoculating 100ml of growth medium (see below) with 0.2ml of stock culture and incubating this at 37°C under vacuum without stirring. After 12–16h the supernatant liquid was decanted, and the sediment of cells was used to inoculate 1litre of the medium of Cohen & Rickenberg (1956) containing KNO_3 (0.5%, w/v), vitamin-free casamino acids (casein hydrolysate) (0.1%, w/v), either glycerol (0.5%, w/v) or potassium succinate (0.5%, w/v) and, in experiments where cells de-repressed for formate oxidation were required, 1 μM-$(NH_4)_6Mo_7O_{24}$ and 1 μM-K_2SeO_3. The medium had been made anoxic before inoculation by bubbling it with O_2-free N_2 in a stirred fermenter for 24h. After inoculation, growth was allowed to proceed for 12–16h at 37°C and controlled at pH7.0. Bacteria were harvested at 0–4°C by centrifugation at 7000*g* for 15min in the 6×750ml head of a Mistral 6L centrifuge (MSE, Manor Royal, Crawley, Sussex, U.K.) and washed twice in the medium of Cohen & Rickenberg (1956), which, in the absence of further additions, is essentially 88mM-potassium phosphate buffer, pH7.3, containing 15mM-$(NH_4)_2SO_4$ and trace elements. We used this medium for suspending cells in some experiments, and refer to it as phosphate buffer.

The haem-deficient mutant A1004a was grown anaerobically with glucose and nitrate in the large-scale culture described by Kemp *et al.* (1975), without addition of 5-aminolaevulinic acid.

Preparation of spheroplasts

Harvested bacteria were washed twice by centrifugation and resuspension in 10mM-Tris–HCl buffer, pH8.0, at 5°C and resuspended to a final concentration of 1g wet wt. in 40ml of 30mM-Tris–HCl buffer, pH8.0, in 0.6M-sucrose at room temperature (22–24°C); 0.1M-EDTA (Tris salt, pH8.0) was added to give a final concentration of 10mM. The suspension was gently shaken at 30°C in a water bath for 5min. Lysozyme (EC 3.2.1.17) was added to a concentration of 1mg/ml and the suspension was shaken for a further 30–40min at 30°C. This procedure converts the *E. coli* into spheroplasts, which were harvested by centrifugation at 5000*g* for 3min at 4°C in the 8×50ml head of an MSE High-Speed 18 centrifuge. The pellet was washed twice in 0.6M-sucrose–5mM-$MgCl_2$ and finally resuspended at a protein concentration of 20–30mg/ml in 0.3M-sucrose–0.15M-KCl–3mM-$MgCl_2$–1.5mM-glycylglycine, pH6.8, at 0–4°C. We refer to spheroplasts as such and to untreated cells as 'cells'.

Other methods

Protein was assayed as described by Lowry *et al.* (1951). Oxygen-uptake rates of cells were measured with an oxygen electrode (type YS1 4004; Yellow Springs Instrument Co., Yellow Springs, Ohio 45387, U.S.A.), and calibrated as described by Chappell (1964). Procedures for the measurement of proton translocation, osmotic swelling and measurement of changes in the reduction of cytochrome *b* are described in the legends to the Figures.

Determination of nitrate uptake by haem-deficient mutant A1004a

The procedure of Wilson & Pardee (1962) was followed, and the cytoplasmic water of a centrifuged wet pellet of cells was determined from the difference between the total water and the FMN-permeable space of the pellet. Nitrate was assayed by a modification of the nitrate reductase assay method described by Ruiz-Herrera *et al.* (1969). The nitrate uptake of cells was measured after 5min incubation at 30°C in aerobic 50mM-KH_2PO_4–Na_2HPO_4 buffer, pH6.8, containing 1.0mM- or 5.0mM-KNO_3 at 30°C. These experiments were performed by Dr. M. B. Kemp.

Reagents

Carbonyl cyanide *m*-chlorophenylhydrazone was from Calbiochem, London W1H 1AS, U.K. Valinomycin and lysozyme chloride (grade VI) were from Sigma Chemical Co., Kingston-upon-Thames KT2 7BH, Surrey, U.K. Nigericin was from Eli Lilly and Co., Indianopolis, Ind. 46206, U.S.A. Carbonate

dehydratase (EC 4.2.1.1) from ox erythrocytes was kindly given by Dr. J. C. Kernohan. All other reagents were of A.R. grade where obtainable. Vitamin-free casamino acids were purchased from Difco Laboratories, Detroit, Mich., U.S.A.

Results and Discussion

Rates of respiratory-driven proton translocation by spheroplasts of anaerobically grown E. coli derepressed for nitrate reductase

Fig. 1 shows pH changes observed when anaerobic suspensions of spheroplasts were permitted brief bursts of respiration in response to small additions of oxygen or nitrate. The changes followed a time-course similar to those described by Lawford & Haddock (1973) for aerobically grown *E. coli* responding to small additions of oxygen. Immediately after addition of oxygen or nitrate there was a rapid phase of acidification, too fast to resolve with a conventional pH-meter and pen-recorder, and this was followed by a slow first-order decay back to the original value with a half-time of about 1 min. Some preparations of spheroplasts exhibited rather different decay kinetics, with a much faster decay and sometimes a considerable excess of the extent of the fast phase of acidification over the completed extent of the subsequent alkalinization phase. Such preparations were not used for measurements of $\rightarrow H^+/2e^-$ stoicheiometries. The fast but short-lived phase of acidification following additions of nitrate show that, despite the relatively high K_m of membrane-bound or purified nitrate reductase for nitrate [about 0.5mM according to Forget (1974), using a manometric assay, and 0.2mM in our own laboratory, using a spectrophotometric assay], it is still possible to use nitrate as a pulse oxidant in the same way as oxygen (Mitchell & Moyle, 1967) or quinones (Lawford & Garland, 1972) have been used in other systems. Addition of the proton-conducting agent carbonyl cyanide *m*-chlorophenylhydrazone (Heytler, 1963) caused rapid acceleration of the decay phase. Subsequent additions of nitrate did not cause acidification.

The rates of the brief bursts of proton translocation described here cannot be measured with conventional commercial pH-meters and pen-recorders, where the overall response time (defined as the time taken for the apparatus to respond to $1 - e^{-1}$, or 0.63, of a step change in the variable measured) is about 2s. By using a fast-responding pH-meter and a storage-oscilloscope for display, the response time of our pH-measuring apparatus falls to 0.4s, and is limited by the mixing time. The recordings shown in Fig. 2 have been drawn by direct tracing over oscilloscope photographs, and show several important features of the proton translocation associated with nitrate

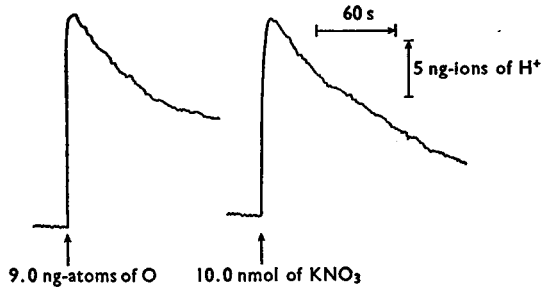

Fig. 1. *pH recordings of proton translocation in response to small additions of oxygen or nitrate to anaerobic spheroplasts of E. coli*

Cells were grown anaerobically in the presence of succinate and nitrate, and converted into spheroplasts as described in the Materials and Methods section. The pH-measuring apparatus has a final incubation volume of 1.0ml and was as described by Lawford & Garland (1972). Spheroplasts (2.4mg of protein) were suspended in 1.0ml of N_2-saturated 0.3M-sucrose–150mM-KCl–1.5mM-glycylglycine buffer, pH7.0, at 30°C containing valinomycin (5μg/ml) and 1mM-potassium succinate. After about 10min of incubation, during which time the pH was maintained between 6.8 and 7.0 by small additions of 50mM-KOH in 100mM-KCl, 20μl of air-saturated 150mM-KCl (oxygen content taken to be 0.45μg-atom/ml) or 2μl of N_2-saturated 5.0mM-KNO_3 in 100mM-KCl were injected into the suspension with a micro-syringe. The moments of injection are shown with arrows in the Figure. The response of the pH electrode to changes of H^+ concentration in the bulk phase was determined by injecting 2μl of N_2-saturated 5mM-HCl in 150mM-KCl into the suspension.

reduction. First, proton translocation commences without any marked delay after injection of nitrate. Obviously in a mixing-limited system with a response time of 0.4s there will be a delay such that, if a linear rate of proton translocation were to be established on complete mixing, then the observed rate at 0.4, 0.8, 1.2 and 1.6s respectively would be 63%, 87%, 95% and 98.2% of the fully mixed rate if it is assumed that mixing is exponential. Secondly, there is not a preliminary alkalinization phase before proton translocation that could be attributed to NO_3^-–OH^- exchange across the cytoplasmic membrane. Such an alkalinization could not in any case be very large. If the cytoplasmic water of spheroplasts were 10μl/mg of protein then in the experiments of Fig. 2 equilibration of NO_3^- by a NO_3^-–OH^- exchange between the extra- and intra-cellular compartments would have released approx. 0.7ng-ion of H^+ in trace (*a*) and 0.12ng-ion of H^+ in trace (*e*). Although these changes are not so small as to be undetectable, they could be masked by acidification due to proton translocation.

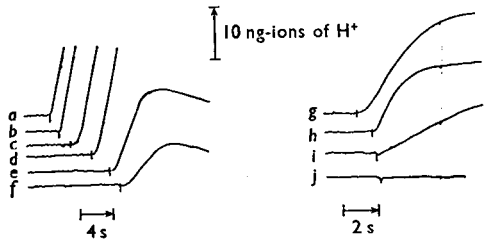

Fig. 2. *Effect of azide and of variation of nitrate concentration on the rate of proton translocation by spheroplasts*

The experiments were performed similarly to those of Fig. 1, except that a pH-meter with a response time set at 20ms was used with a storage-oscilloscope. The oscilloscope display was photographed and tracings were made of the recording and stacked as in the Figure for convenience. In the left-hand set (*a–f*) the protein concentration was 2.3mg/ml and the added reductant was 1mM-L-malate. In the right-hand set (*g–j*) the protein concentration was 1.4mg/ml and the reductant was 2mM-succinate. A small deflexion on each trace identifies the moment of injection of small amounts of N_2-saturated 5mM-KNO_3 in 150mM-KCl. The initial concentrations of nitrate on injection were (*a*) 30μM, (*b*) 20μM, (*c*) and (*d*) 10μM, (*e*) 5μM, (*f*) 2.5μM and (*h*) and (*j*) 10μM. In traces (*g*) and (*i*) 9.0ng-atoms of oxygen were injected as 20μl of air-saturated 150mM-KCl. In traces (*i*) and (*j*) 0.4mM-NaN_3 was also present. Injection of solutions with a micro-syringe gave a small vertical deflexion on the oscilloscope recording, and this deflexion times the moment of injection.

However, alternative evidence against the existence of an NO_3^-–OH^- exchange is presented below. Thirdly, the rate of proton translocation increased with nitrate concentration up to 20μM-nitrate, beyond which the rate did not further increase. This indicates that the apparent K_m of nitrate reductase for reduction of nitrate by the respiratory chain is at least tenfold less than that when the reductant is reduced Benzyl Viologen. Fourthly, 0.4mM-azide completely abolished proton translocation coupled to nitrate reduction, whereas that coupled to oxygen reduction was only 50% inhibited.

The absolute rate of proton translocation coupled to nitrate reduction in Fig. 2(*e*) was 94ng-ions of H^+/min per mg of protein. The average rate of nitrate reduction calculated from the amount of nitrate added (5nmol) and the duration of the acidification phase (equated with duration of nitrate reduction) was 25nmol/min per mg of protein. Thus the ratio of the rates of proton translocation and nitrate reduction was 3.76, which is in reasonable agreement with the stoicheiometry measurements.

Table 1. *Ratios for $\rightarrow H^+/NO_3^-$ and $\rightarrow H^+/O$ for spheroplasts of E. coli grown anaerobically with glycerol and nitrate*

Experimental conditions were as shown in Fig. 1, except that potassium succinate was replaced with 2mM-L-malate or -D-lactate or -formate as their potassium salts, or 2mM-glycerol. The values for $\rightarrow H^+/2e^-$ are for the means (±S.E.M.) for several observations (numbers in parentheses) made on the same preparation with small additions of nitrate giving concentrations of 5μM-, 10μM- and 15μM-nitrate, or with air-saturated 150mM-KCl giving oxygen concentrations of 4.5, 9.0 and 13.5ng-atoms of oxygen/ml. The $\rightarrow H^+/2e^-$ ratios in these experiments were independent of the amount of nitrate or oxygen added within the range stated. In all cases the observed peak, and not the extrapolated peak, of acidification was used in the calculations.

Added substrate (2mM)	$\rightarrow H^+/NO_3^-$	$\rightarrow H^+/O$
None	3.4 ±0.2 (6)	3.9 ±0.15 (5)
L-Malate	3.45±0.13 (7)	3.1 ±0.05 (7)
D-Lactate	1.9 ±0.06 (8)	1.9 ±0.05 (5)
Glycerol	2.1 ±0.07 (7)	2.2 ±0.07 (7)
Formate	1.6 ±0.17 (9)	3.63±0.11 (7)

$\rightarrow H^+/2e^-$ ratios for anaerobically grown E. coli oxidizing oxygen or nitrate

The $\rightarrow H^+/2e^-$ ratios were determined as in the experiments of Fig. 1, and the results are summarized in Table 1. The $\rightarrow H^+/NO_3^-$ ratios were close to the $\rightarrow H^+/O$ ratios, except for formate oxidation. If these values are interpreted according to the ideas of Lawford & Haddock (1973), then they indicate the presence of two energy-conservation sites or regions in the respiratory chain between NADH and nitrate, and only one such site between glycerol or D-lactate and nitrate. These observations confirm and extend the report of Brice *et al.* (1974) that the $\rightarrow H^+/NO_3^-$ ratio for oxidation of endogenous substrates is approx. 4.

Proton translocation associated with formate oxidation

Cells grown anaerobically in the presence of nitrate supplemented with molybdate and selenite develop high activities of formate oxidation by nitrate or oxygen (Enoch & Lester, 1972). Measurements of the $\rightarrow H^+/2e^-$ ratio as for Fig. 1 gave values of 3.63±0.11 (seven observations) for the $\rightarrow H^+/O$ ratio and 1.6±0.17 (nine observations) for the $\rightarrow H^+/NO_3^-$ ratio (Table 1). However, the interpretation of the pH recordings in these experiments was not straightforward. As shown in Fig. 3, the decay of the acidification arising during a burst of formate oxidation was markedly biphasic, and this is clearly seen when a semi-logarithmic plot is used (Fig. 4). There are five processes that must be considered when

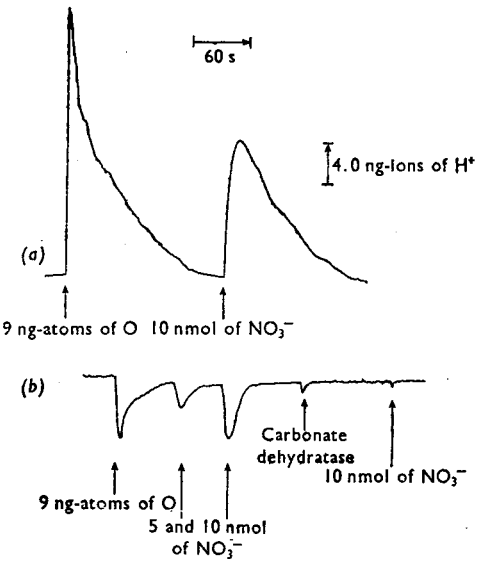

Fig. 3. *pH changes associated with formate oxidation by spheroplasts*

The experiments were carried out essentially as described in Fig. 1, except that cells were grown anaerobically with glycerol as the carbon source, and the growth medium supplemented with 1 μM-$(NH_4)_6Mo_7O_{24}$ and 1 μM-K_2SeO_3 as well as nitrate (see the Materials and Methods section). Potassium formate (3 mM) replaced succinate as the respiratory substrate for proton translocation, but otherwise the conditions were identical. In the lower trace (*b*) 3 μM-carbonyl cyanide *m*-chlorophenylhydrazone was also present. In trace (*a*) the $\rightarrow H^+/2e^-$ ratio at the peak of acidification following oxygen addition was 3.4, and for nitrate it was 1.7. In trace (*b*) the $\rightarrow H^+/2e^-$ ratio at the most alkaline point following oxygen addition was −1.0, and for nitrate it was −0.9. Carbonate dehydratase was added at the point indicated to give a final concentration of 1 μg/ml.

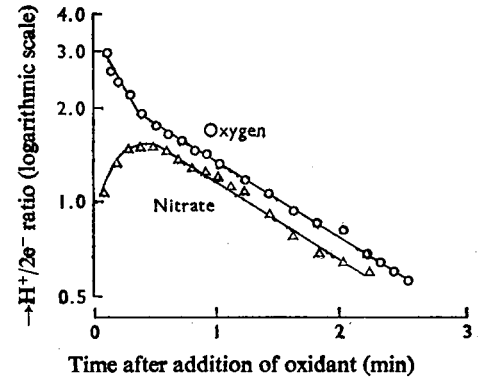

Fig. 4. *Semi-logarithmic plot of pH changes associated with oxidation of formate by oxygen or nitrate*

The data are taken from Fig. 3, and the pH changes have been converted into $\rightarrow H^+/2e^-$ ratios and plotted on a logarithmic scale against time. The decay in the case of oxygen (○) is markedly biphasic, giving $\rightarrow H^+/2e^-$ ratios of 2.3 and 3.6 when extrapolated to zero time. The decay in the case of nitrate (△) is not biphasic, and gives an $\rightarrow H^+/2e^-$ ratio of 1.9 when extrapolated to zero time.

attempting to interpret the kinetics of the recordings of pH changes associated with formate oxidation by oxygen:

$$H^+ + HCO_2^- \rightleftharpoons HCO_2H \quad (1)$$

$$HCO_2H_{extracellular} \rightleftharpoons HCO_2H_{intracellular} \quad (2)$$

$$H^+ + HCO_2^- + \tfrac{1}{2}O_2 \rightarrow H_2O + CO_2 \quad (3)$$

$$H_2O + CO_2 \rightleftharpoons H_2CO_3 \quad (4)$$

$$H_2CO_3 \rightleftharpoons H^+ + HCO_3^- \quad (5)$$

The first and last of these processes are effectively instantaneous acid dissociations with pK values of 3.62 and 3.77 respectively. The second process is the diffusion of formic acid from the extracellular to intracellular space, and its rate was too fast to measure in hand-mixed osmotic-swelling experiments. Formate anion does not diffuse readily across the cytoplasmic membrane (see below). The distribution of formate across the cytoplasmic membrane will therefore be determined by the relationship:

$$\frac{[\text{formate}]_{in}}{[\text{formate}]_{out}} = \frac{[H^+]_{out}}{[H^+]_{in}}$$

where 'in' and 'out' refer respectively to the intracellular and extracellular spaces separated by the cytoplasmic membrane.

Respiratory-driven proton translocation in the presence of valinomycin and K^+ effects a H^+–K^+ exchange across the cytoplasmic membrane, creating a pH gradient that is acid extracellularly. This will displace formic acid from the extracellular to the intracellular space, and may well account for the fast early phase of the biphasic decay seen in Figs. 3 and 4.

A further complexity arises from the consumption of a proton in the overall formate oxidase reaction, the third process listed above. The consumption of protons in this process must be simultaneous in the time-scale of these experiments with the burst of formate oxidation, and could contribute to the slower decay process only if the site for formate oxidation were on the inner aspect of the cytoplasmic membrane. This could not explain the biphasic decay kinetics except through the uptake of formic acid as just described. The consumption of 1 g-ion of H^+/mol

of formate oxidized was demonstrated in the presence of carbonyl cyanide *m*-chlorophenylhydrazone (4 μM) by observation of an $\rightarrow H^+/O$ ratio close to -1.0 (Fig. 3). The alkalinization occurring during the burst of formate oxidation was short-lived, and, as shown in Fig. 3, abolished by the inclusion of carbonate dehydratase (1 μg/ml). This shows that, in the absence of carbonate dehydratase, the hydration of CO_2 was too slow to interfere with the peak of acidification caused by the burst of formate oxidation.

These considerations show that the measured $\rightarrow H^+/O$ ratio for formate oxidation is a minimal estimate. Although a semi-logarithmic plot indicates that the observed value approaches 4.0, the true value would have to be 5.0 if the proton-consuming formate oxidase reaction (process 3) were on the outer aspect of the cytoplasmic membrane. The inclusion of carbonate dehydratase (1 μg/ml) did not increase the peak of acidification observed during a burst of formate oxidation, although it alters the overall formate oxidation reaction (3) during the burst to become:

$$HCO_2^- + \tfrac{1}{2}O_2 \rightarrow HCO_3^-$$

It follows that the $\rightarrow H^+/O$ ratio for formate oxidation approaches 4, not 5, and that formate is oxidized on the inner aspect of the cytoplasmic membrane.

The $\rightarrow H^+/2e^-$ ratio for formate oxidation by nitrate did not exceed 2.0. Comparison of the kinetics of the pH changes with oxygen or nitrate as the oxidant for formate showed that the rate of proton translocation associated with formate oxidation by oxygen was about 1500 ng-atoms of H^+/min per mg, whereas that for oxidation by nitrate was about tenfold less. The relatively slower rise of the peak of acidification in the case of nitrate could be obscured by a fast decay phase of alkalinization, with the result that the peak value corresponding to the true $\rightarrow H^+/NO_3^-$ ratio is not seen (Figs. 3 and 4). Unfortunately, there is no means of knowing whether this is the case or not, and so the true $\rightarrow H^+/NO_3^-$ ratio may approximate to 2 as observed or may, by analogy with the $\rightarrow H^+/O$ ratio for formate oxidation by oxygen, approach 4.

Mechanism of proton translocation associated with reduction of nitrate

A number of proposals have been made for the mechanism of respiratory-driven proton translocation (Greville, 1969). Scheme 1(*a*) shows the respiratory carriers of *E. coli* from ubiquinone to nitrate reductase (Enoch & Lester, 1974) arranged to yield a proton-translocating loop of the type envisaged by Mitchell (1966). An essential feature of this scheme is that the nitrate-reducing site is on the inner aspect of the cytoplasmic membrane. Nitrate must therefore cross the membrane at a rate no less than the observed rate of nitrate reduction. In addition, inhibitors of nitrate reductase that compete with nitrate must also cross the membrane. We have tested these two predictions by measuring the rate of nitrate entry into spheroplasts and the distribution of nitrate between cells and the medium, and by studying the characteristics of inhibition by azide of nitrate reductase in cells and spheroplasts.

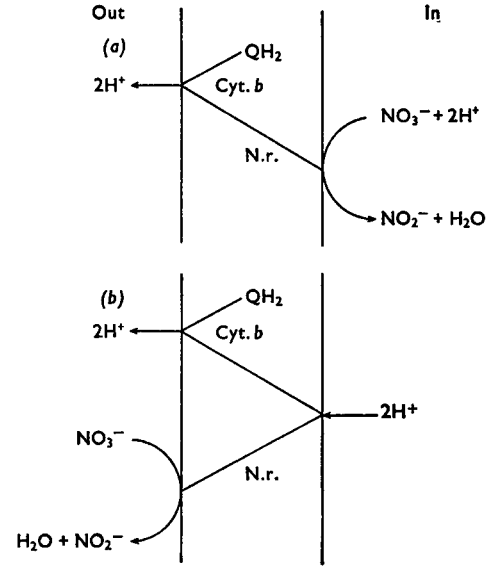

Scheme 1. *Proton-translocating oxidoreduction schemes for nitrate reductase*

These schemes are based on analogous schemes for respiratory-driven proton translocation in mitochondria (Mitchell, 1966), and the sequence of respiratory carriers in *E. coli* from ubiquinol to nitrate shown by the reconstitution studies by Enoch & Lester (1974). The pair of vertical lines represents the cytoplasmic membrane, and 'out' and 'in' refer to the extracellular and intracellular spaces respectively. The diagonal lines represent the pathways of electron or hydrogen transfer. Two schemes are shown. Cytochrome *b* (Cyt. *b*) acts in each as an electron carrier. Nitrate reductase (N.r.) acts as an electron carrier in scheme (*a*). In scheme (*b*) nitrate reductase is drawn as a vectorial enzyme; it effectively acts as a transmembrane hydrogen carrier, irrespective of whether the protons and electrons traverse the membrane together or in spatially distinct paths. In each scheme QH_2 stands for reduced quinone, which could be menaquinone or ubiquinone. The relative contribution of each in the flow of reducing equivalents from respiratory substrate to nitrate is unknown.

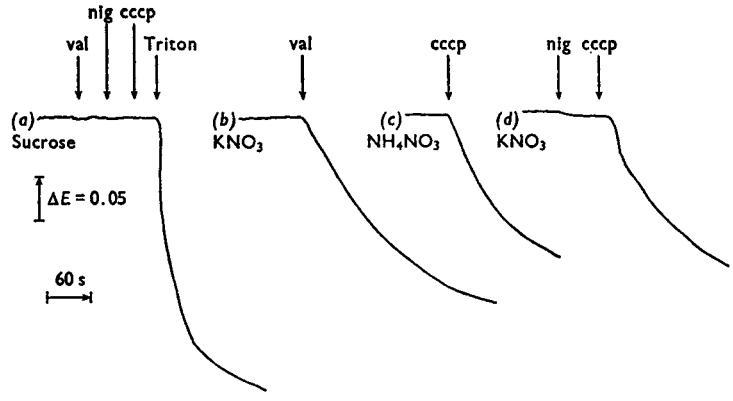

Fig. 5. *Osmotic behaviour of spheroplasts in iso-osmotic solutions of nitrate salts*

Spheroplasts were prepared as described in the Materials and Methods section and resuspended at a concentration of 25mg of protein/ml in 0.5M-sucrose–10mM-glycylglycine buffer, pH7.0, and kept at 0°C. Osmotic swelling was followed spectrophotometrically in a cuvette of 1cm light-path by recording the extinction at 500nm on the addition of 25μl of the spheroplast suspension to 2.5ml of an iso-osmotic solution of various solutes at 30°C. When added to 0.5M-sucrose the extinction value was approx. 0.5, whereas the value in water was approx. 0.15. Valinomycin (val) and nigericin (nig) were added as 2.5μl additions of methanolic solutions (1mg/ml), carbonyl cyanide *m*-chlorophenylhydrazone (cccp) as 2.5μl of a methanolic 3mM solution, and Triton X-100 as 10μl of an aqueous 1% solution. The iso-osmotic solutions were (*a*) 0.5M-sucrose, (*b*) and (*d*) 0.25M-KNO_3 and (*c*) 0.25M-NH_4NO_3.

Measurement of nitrate entry into spheroplasts

There are but few reports of the rates of nitrate uptake into micro-organisms, probably because of the lack of radioactive nitrate. We have used an indirect method of measuring rates of nitrate penetration, based on the osmotic sensitivity of spheroplasts (Sistrom, 1958). Figs 5 and 6 show the extinction changes occurring at 500nm when spheroplasts were suspended in various solutions that were iso-osmotic with the cytoplasm of *E. coli* spheroplasts. These experiments, and others similar but not shown, determined qualitatively the permeability characteristics of the cytoplasmic membrane of spheroplasts towards various solutes. The interpretation of the spectrophotometer records of Fig. 5 is as follows. It is shown in Fig. 5(*a*) that iso-osmotic sucrose provides osmotic support, and that valinomycin, nigericin or carbonyl cyanide *m*-chlorophenylhydrazone do not lyse spheroplasts at the concentrations used, whereas the detergent Triton X-100 does. In Fig. 5(*b*) it is shown that iso-osmotic KNO_3 provides osmotic support. Swelling occurred after the addition of valinomycin, which effects electrogenic K^+ movement across the cytoplasmic membrane (Harold, 1970). The membrane must therefore also be crossed by NO_3^-. Fig. 5(*c*) shows that iso-osmotic NH_4NO_3 provides osmotic support. By contrast, iso-osmotic ammonium acetate or ammonium formate did not provide osmotic support (results not shown), whereas the potassium salts did so even in the presence of valinomycin (1μg/ml). It can therefore be concluded that the cytoplasmic membrane is permeable to NH_3, and to acetic acid and formic acid but not their anions. It can also be concluded that an electroneutral transport mechanism involving NO_3^-–OH^- exchange was not operative, although such a mechanism was artifically set up when the proton conductor carbonyl cyanide *m*-chlorophenylhydrazone was added to iso-osmotic NH_4NO_3. Further evidence against a nitrate-transport system involving NO_3^-–OH^- exchange was provided by the experiment of Fig. 5(*d*), where addition of nigericin, which effects an electroneutral H^+–K^+ exchange (Harold, 1970), did not cause swelling of spheroplasts in iso-osmotic KNO_3. However, further addition of carbonyl cyanide *m*-chlorophenylhydrazone did cause swelling, because in combination with nigericin it mimics valinomycin in facilitating electrogenic K^+ movement across the membrane.

Swelling of spheroplasts in iso-osmotic NH_4NO_3 was mainly complete in less than 5s, showing that at least for swelling slower than this the movement of solute, not water, is rate-limiting for swelling. The rate of swelling induced by addition of valinomycin (2μg/ml) to spheroplasts in iso-osmotic KNO_3 was not stimulated by further increasing the valinomycin concentration up to 10μg/ml. This maximal rate of valinomycin-induced swelling was limited by the rate of NO_3^- movement across the membrane, because this rate was identical with that induced

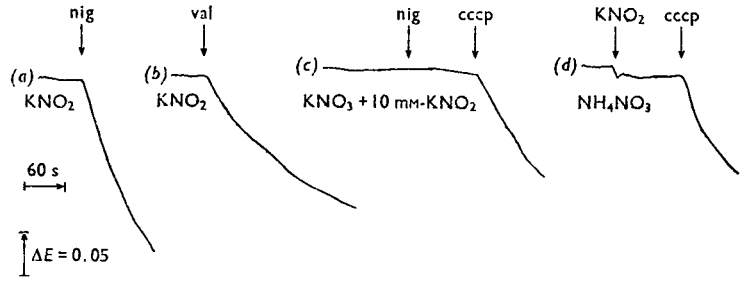

Fig. 6. *Osmotic behaviour of spheroplasts in the presence of nitrite salts*

The conditions were as described for Fig. 5. The iso-osmotic solutions were (*a*) and (*b*) 0.25 M-KNO_2, (*c*) 0.25 M-KNO_3 and (*d*) 0.25 M-NH_4NO_3. In (*c*) and (*d*) KNO_2 was added as 0.1 ml of 0.25 M-KNO_2 to give a final concentration of approx. 10 mM.

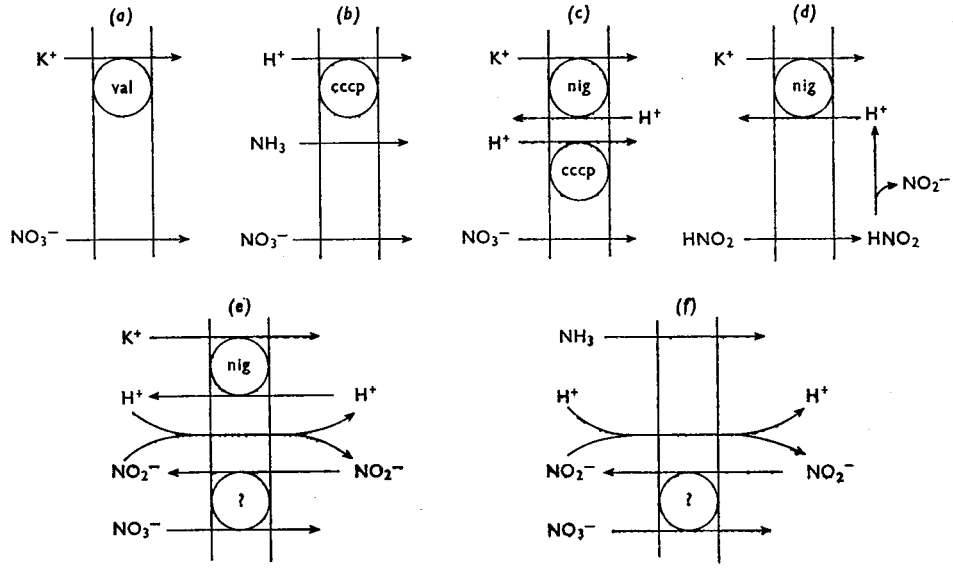

Scheme 2. *Pathways for entry of potassium nitrate, ammonium nitrate or potassium nitrite into spheroplasts*

In each scheme from (*a*) to (*f*) the pair of vertical lines represents the cytoplasmic membrane with the cytoplasm on the right and extracellular space on the left. Large circles in the membrane represent specific pathways provided by valinomycin (val) for K^+, carbonyl cyanide *m*-chlorophenylhydrazone (cccp) for H^+, nigericin (nig) for K^+–H^+ exchange, and a hypothetical NO_3^-–NO_2^- exchange system (?). Passive diffusion is shown for NO_3^-, NH_3 and HNO_2. These schemes variously would facilitate entry into spheroplasts of KNO_3 [(*a*), (*c*) and (*e*)], NH_4NO_3 [(*b*) and (*f*)] and KNO_2 [(*d*), and also (*a*) if NO_2^- is substituted for NO_3^-]. In schemes (*e*) and (*f*), the major anion is NO_3^- and the role of NO_2^- is to cycle between the intra- and extra-cellular spaces.

by carbonyl cyanide *m*-chlorophenylhydrazone in iso-osmotic NH_4NO_3 (Fig. 5*c*) or by carbonyl cyanide *m*-chlorophenylhydrazone with nigericin in iso-osmotic KNO_3 (Fig. 5*d*). In the latter experiment (Fig. 5*d*) the rate of swelling was not increased further by adding valinomycin (2 μg/ml) along with carbonyl cyanide *m*-chlorophenylhydrazone.

Measurements of nitrite entry into spheroplasts

The permeability of the cytoplasmic membrane towards nitrite was investigated in the experiments of Fig. 6. Either nigericin or valinomycin caused swelling of spheroplasts in iso-osmotic KNO_2, from which it can be concluded that both HNO_2 (p*K* 3.34)

and NO_2^- anion can cross the membrane. The possible existence of a transport system for nitrate involving NO_3^-–NO_2^- exchange was sought in the experiments of Figs. 6(*c*) and 6(*d*). In Fig. 6(*c*) the combination of nigericin-mediated K^+–H^+ exchange with HNO_2 diffusion would have produced swelling if an NO_3^-–NO_2^- exchange were also operative, but in fact did not. Less crucially, swelling in iso-osmotic NH_4NO_3 initiated on adding carbonyl cyanide *m*-chlorophenylhydrazone (Fig. 5*d*) was no faster if 10mM-KNO_2 was also present (Fig. 6*d*), whereas it would have been if an NO_3^-–NO_2^- exchange was operative. Schemes summarizing the various solute movements involved or sought in these experiments are drawn in Scheme 2.

Rate of nitrate entry into spheroplasts

NO_3^- is a relatively lipophilic anion, and the demonstration that it could cross the cytoplasmic membrane was not unexpected. Nevertheless the rate at which nitrate must enter in the nitrate reductase assay with reduced Benzyl Viologen in spheroplasts is high, because the maximal activity of the enzyme when fully de-repressed is between 2 and 5 μmol of nitrate reduced/min per mg of protein (Kemp *et al.*, 1975). We have used the rates of osmotic swelling of spheroplasts when maximally stimulated by valinomycin to calculate the rate of nitrate entry by what we take to be passive diffusion. The procedure is based on that of Sistrom (1958), and assumes that spheroplasts, as any osmometer, respond only to an osmotic-pressure difference across the membrane; an increase in the internal osmotic pressure will cause the same extent of swelling as does an identical decrease externally. By using this assumption Sistrom (1958) was able to determine, from the extent of osmotic swelling, the uptake of β-D-thiogalactoside by spheroplasts of *E. coli*. The value so obtained was in reasonable agreement with the value determined by uptake of radioactive β-D-thiogalactoside. We were encouraged by this to use a similar approach to determine the rate rather than extent of solute uptake. To do this it was necessary to record the initial rate of valinomycin-induced swelling and also the final extent of swelling of spheroplasts over a range of KNO_3 concentrations. The other solute was K_2SO_4, and the final osmolarity was constant at 0.5osM. The results are summarized in Fig. 7.

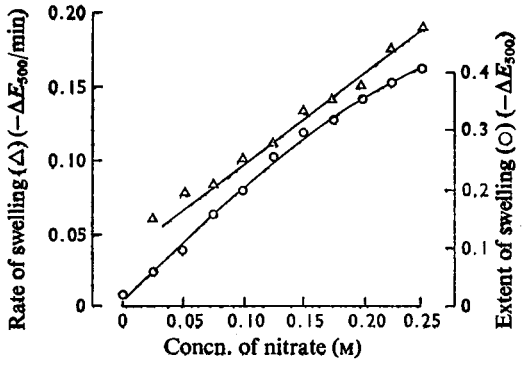

Fig. 7. *Dependence on nitrate concentration of the rate and extent of valinomycin-induced swelling of spheroplasts*

Spectrophotometric measurements of the rate and extent of valinomycin-induced swelling of spheroplasts were made essentially as described in Fig. 5, except that the final concentration of spheroplasts in 2.5ml was 1.0mg of protein/ml and swelling was initiated by adding 5 μl of a methanolic solution of valinomycin (1mg/ml). The NO_3^- concentration was varied by mixing KNO_3 with K_2SO_4 to maintain a final osmolarity of 0.5osM.

Fig. 7 shows that both the rate and the extent of swelling are related to the initial difference of nitrate concentration across the membrane, if we assume negligible uptake of KNO_3 in the absence of valinomycin. The slope of the curve relating the extent of swelling to initial concentration difference of nitrate across the membrane was between 1 and 2 E_{500} units·M^{-1}. Taking the mean value of 1.5 E_{500} units·M^{-1}, the relationship between rate of swelling and the initial concentration difference of nitrate across the membrane (0.75 E_{500} unit·min^{-1}·M^{-1} from Fig. 7) can be converted into the rate of change of concentration difference of nitrate for a given concentration difference, which we calculate to be 0.5min^{-1} (i.e. 0.75 E_{500} unit·min^{-1}·M^{-1} divided by 1.5 E_{500} units·M^{-1}). At constant extracellular nitrate concentration the change of concentration difference across the membrane is equal to the change of intracellular nitrate concentration. Hence the rate of nitrate penetration into a given volume of intracellular water can be calculated.

If we assume that the spheroplast is a sphere of diameter 1 μm, then the permeability coefficient of the cytoplasmic membrane at 30°C is 1.4×10^{-10}cm·s^{-1}. In making this calculation we ignored changes in the nitrate concentration of the medium due to nitrate uptake, and changes of the spheroplast volume: neither error can be very significant at the onset of valinomycin-induced swelling. Another calculation of interest can be made if we assume that there is 10 μl of cytoplasmic water/mg of spheroplast protein. As shown above, the cytoplasmic concentration of nitrate changes by 0.5M/min for a 1.0M concentration difference across the membrane. This yields a rate of nitrate entry of 5.0 μmol/min per mg of spheroplast protein for a 1.0M concentration difference of nitrate across the cytoplasmic membrane. At an extracellular nitrate concentration of 0.2mM, which corresponds to the K_m of nitrate

reductase activity for nitrate, the maximal calculated rate of nitrate entry by passive diffusion obeying Fick's Law (Fick, 1855) would be 1.0nmol/min per mg. This rate is about 0.1% of that required to support the observed rate of nitrate reductase of spheroplasts at the K_m for nitrate.

Is there a transport system for nitrate?

The osmotic-swelling method for determining rates of nitrate penetration into spheroplasts became inaccurate at nitrate concentrations of 0.05M or less, because the spectrophotometric changes were small. A transport system would not obey Fick's Law, and a low K_m value for nitrate could ensure as high a rate of nitrate entry at, say, 0.05mM- as at 0.05M-nitrate. However, the lower range of rates of nitrate entry measured by osmotic swelling was about 1.25μmol/min per mg of protein, and all of this rate would be required to support observed rates of nitrate reductase. Thus, even if osmotic swelling did include a nitrate-transport system of low K_m, the conclusion that the only significant pathway of nitrate entry was by electrogenic movement of nitrate anion is still valid, irrespective of whether the pathway was by passive or facilitated diffusion. A transport system for the electrogenic uptake of NO_3^- anion would meet a considerable difficulty from the electrical potential across the cytoplasmic membrane, which has been estimated to be −140mV in EDTA-treated cells of *E. coli* (Griniuviene *et al.*, 1974) and −125mV in right-side-out vesicles of *E. coli* (Altendorf *et al.*, 1975). This membrane potential would act to exclude nitrate from the cytoplasm, resulting in a cytoplasmic nitrate concentration less than 1% of that extracellularly. We investigated the distribution of nitrate between cellular and extracellular water of *E. coli*, essentially by the methods of Wilson & Pardee (1962) and using FMN as a marker molecule for the extracytoplasmic space. The FMN-impermeable space was therefore equated with the cytoplasm. To avoid further metabolism of nitrate we used a haem-less mutant of *E. coli* that was de-repressed for nitrate reductase but unable to reduce nitrate at measurable rates unless reduced Benzyl Viologen was supplied (Kemp *et al.*, 1975). Added nitrate (1 or 5mM) was quantitatively recovered from suspensions and centrifuged pellets of these cells. It was found that the nitrate-permeable space of *E. coli* was about 30–50% of the cytoplasmic space, and that this space fell to undetectable size (<20% of the cytoplasmic space) in the presence of glucose (28mM) as an energy source. In view of the inaccuracies inherent in measuring a small and incompletely permeated intracellular space, we did not pursue this investigation further, and it is not reported in detail. Nevertheless, we can conclude that there is not an active transport system for nitrate in *E. coli* cells that have been de-repressed for nitrate reductase.

Entry of azide into spheroplasts and the site of its action on nitrate reductase

Azide is a potent inhibitor of membrane-bound and purified nitrate reductase, competing against nitrate with a K_i of 2–5μM when assayed manometrically (Forget, 1974) or 0.2μM when assayed spectrophotometrically (J. A. Downie, unpublished work). Osmotic swelling experiments (not shown) demonstrated that hydrazoic acid (pK 4.7) penetrated spheroplasts very rapidly, whereas azide penetrated more slowly. This is consistent with the uncoupling (equated with proton-conducting) properties of azide, which are exhibited at high (10mM) but not low (10μM) concentrations. Since azide is the anion of a weak lipophilic acid, its distribution across a membrane will be determined by the transmembrane pH differential. This behaviour was exploited by Palmieri & Klingenberg (1967) to show that the azide-sensitive site of mitochondrial cytochrome oxidase (EC 1.9.3.1) is located on the inner aspect of the inner mitochondrial membrane. We have used a similar approach to determine whether treatments expected to set up or modify a pH differential across the cytoplasmic membrane of *E. coli* affected the inhibitory action of azide on nitrate reductase. We use an indirect but convenient assay for measuring nitrate reductase activity. Advantage was taken of the fact that the addition of small amounts of nitrate to a suspension of *E. coli* provided with a respiratory substrate such as L-malate will cause brief cycles of cytochrome *b* oxidation followed by reduction as the nitrate supply becomes exhausted. The time taken from the onset of cytochrome *b* oxidation by nitrate to the time when cytochrome *b* had half-returned to its previous state of reduction is called the 'cycle time' and was taken as a measure of the nitrate reductase activity. The cycle time gave a time-averaged rate of nitrate reduction for that addition of nitrate. Fig. 8 shows how this was done, and is a series of dual-wavelength spectrophotometer recordings of changes in cytochrome *b* reduction in *E. coli* cells in the presence of 25mM-L-malate. The cell suspension was unstirred and had become anoxic through complete utilization of dissolved oxygen. The top recording in Fig. 8 shows the effect of adding small but increasing amounts of nitrate. In each case cytochrome *b* is immediately oxidized, and there is a small overshoot that is due to the addition of air along with the NO_3^-. Other experiments (not shown) demonstrated that when oxygen and nitrate were added simultaneously then reduction of nitrate did not commence until reduction of oxygen was complete. The cycle time, drawn in Fig. 8 for one of the cycles, was

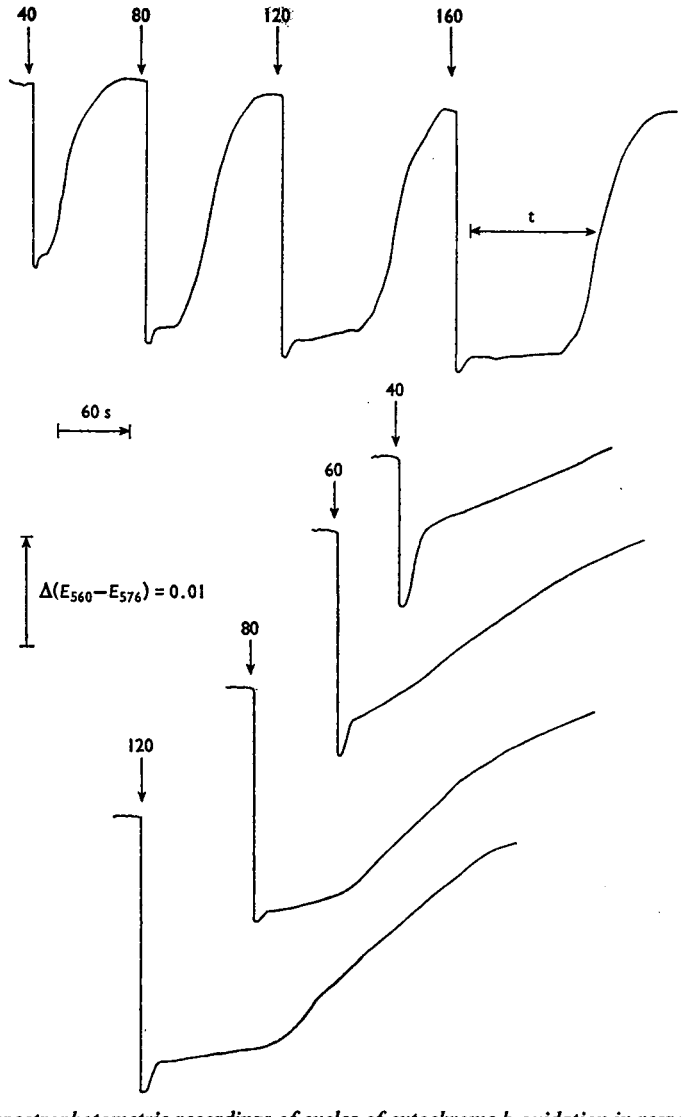

Fig. 8. *Dual-wavelength spectrophotometric recordings of cycles of cytochrome b oxidation in response to small additions of nitrate to cells of anaerobic E. coli*

Bacteria grown anaerobically in nitrate and glycerol medium were washed and resuspended in phosphate buffer, pH7.3, to a final concentration of 30–40mg of protein/ml at 0°C. A 2.5ml volume of the same buffer at 30°C containing 25mM-L-malate as the Tris salt, pH7.3, was used to suspend a portion of stock cell suspension to a final concentration of 4.5mg of protein/ml in a spectrophotometer cuvette of light-path 1cm. The state of reduction of cytochrome *b* was measured with a dual-wavelength spectrophotometer at the wavelength pair 560 and 576nm. An upwards deflexion of the recording in the Figure is due to an increase of extinction at 560nm referred to 576nm, and indicates reduction of cytochrome *b*. In the uppermost recording additions of 0.25M-KNO_3 were made to give initial concentrations of 40μM-, 80μM-, 120μM- and 160μM-nitrate. The horizontal line labelled '*t*' in the final cycle of oxidation shows how the cycle time was measured. The lower four recordings were made in the same way except that 2μM-sodium azide was present, and the initial concentrations of nitrate were 40, 60, 80 and 120μM. The moments of addition of nitrate are shown in the Figure with vertical arrows and the initial nitrate concentration (μM).

considered to start at the end of the initial overshoot due to oxygen. The cycle times in the top recording for additions of nitrate giving initial concentrations of 40μM-, 80μM-, 120μM- and 160μM-nitrate were in the proportions 1:2:3.2:4.2 respectively. This shows, as did the proton-translocation experiments described in Fig. 2, that the physiological rate of reduction of nitrate by the respiratory chain was

saturated by 40 μM-nitrate or less, which is considerably lower than the concentration expected from measurements made with reduced Benzyl Viologen as reductant. The explanation for this lies in the much lower rate of physiological reduction of nitrate (about 20–40 nmol/min per mg of protein in the top recording of Fig. 8 with L-malate as reductant) compared with the rate obtained with reduced Benzyl Viologen. The four lower recordings in Fig. 8 show the effect of a fixed concentration of azide (2 μM) on the cycle time. As expected, graphs of the cycle time (which is proportional to the reciprocal of the average rate of reduction) against the reciprocal of the nitrate concentration in the presence and in the absence of 2 μM-azide showed that the inhibition by azide was competitive with nitrate.

The effect of pH on the inhibitory effectiveness of azide was investigated in the experiment shown in Fig. 9. In this experiment cells stored in 150 mM-KCl were added to suspension medium containing L-malate at pH 5.5, 6.0, 7.0 and 8.0 in the presence and in the absence of 2 μM-azide. Cycle times for nitrate reduction were measured within 10 min of placing the cells in the suspension medium. We do not know the magnitude of any pH difference across the cytoplasmic membrane in these experiments, but it was unlikely to have been identical in magnitude or direction for each of the four different pH conditions of the suspending medium. A transmembrane pH difference of 0.3 will change the intracellular concentration of the anion of a lipophilic acid by a factor of 2 at pH values of more than about 1.0 above the pK value, which for hydrazoic acid is 4.7. Our method would certainly have detected the change in inhibition due to a twofold change of azide concentration. For instance, at 100 μM-nitrate at pH 7.0 in the experiment of Fig. 9, the cycle time was 1.5 min, rising to 3 min at 1 μM-azide, 4.2 min at 2 μM-azide and 5.5 min at 4 μM-azide. No significant changes in the inhibitory effect of azide were observed over the range pH 5.5–8.0 (Fig. 9). We conclude that either any transmembrane pH difference was constant to within about 0.1 pH, which is very unlikely (Kashket & Wong, 1969; White & O'Brien, 1972), or that the azide-sensitive site was on the outer aspect of the cytoplasmic membrane. Further experiments, where the cycle times were measured within 1 min of changing the extracellular pH from 7.0 to 6.0, also failed to show any change in the inhibitory effect of azide.

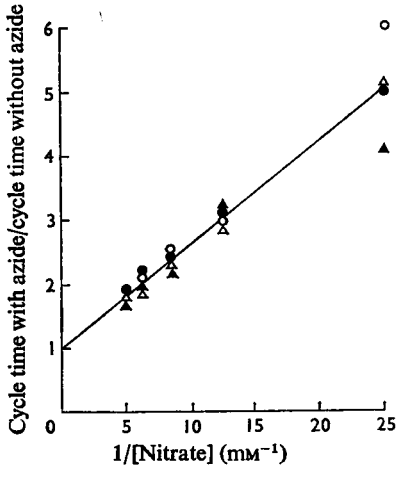

Fig. 9. *Inhibition of nitrate reductase activity of E. coli cells by azide at pH 5.5–8.0*

The Figure shows a graph of the ratio of the cycle time for cytochrome *b* oxidation by small additions of nitrate, in the presence or in the absence of 2 μM-sodium azide, plotted against the reciprocal of the nitrate concentration. The experimental conditions were essentially as described for Fig. 8, except that the buffer was adjusted to pH 5.5 (○), 6.0 (▲), 7.0 (●) and 8.0 (△) with HCl or KOH. The cycle times either in the absence or in the presence of azide were not significantly altered by pH over the range pH 5.5–8.0. The final concentrations of KNO_3 were 40, 80, 120, 160 and 200 μM, and the absolute durations of the cycle times were identical with those given for comparable cycles in Fig. 8. The line drawn in the graph is that predicted for competitive inhibition by azide with respect to nitrate, and shows zero inhibition at infinite nitrate concentration.

We also investigated the effects of valinomycin (4 μg/ml) and carbonyl cyanide *m*-chlorophenylhydrazone (2 μg/ml) on the cycle times for nitrate reduction by spheroplasts in a suspension medium containing 0.3 M-sucrose–0.15 M-KCl–10 mM-glycylglycine buffer, pH 7.0, at 30°C. With 8 mM-formate as substrate and additions of 400 μM-nitrate (initial concentration), the cycle time was doubled by the inclusion of 2 μM-azide irrespective of the presence or absence of valinomycin or carbonyl cyanide *m*-chlorophenylhydrazone. Thus, unlike mitochondria and cytochrome oxidase (Palmieri & Klingenberg, 1967), there is no evidence with *E. coli* and nitrate reductase that azide crosses the respiratory-chain-containing membrane to the azide-sensitive site.

Conclusion

Whatever the mechanism of proton translocation coupled to nitrate reduction, it must account for the observed stoicheiometries for the $\rightarrow H^+/2e^-$ ratio, and also for the consumption of two protons in the reduction of nitrate to nitrite. A possible mechanism is shown in Scheme 1(*b*), and is consistent with the observed proton movements and also the apparent location of the nitrate reducing site of nitrate reductase on the outer aspect of the cytoplasmic membrane. An essential feature of the

scheme is that nitrate reductase is vectorial, and this would be in keeping with the finding that the $FMNH_2$-reducible site of nitrate reductase is located on the inner aspect of the cytoplasmic membrane (Kemp *et al.*, 1975). In this scheme nitrate reductase would effectively act as a hydrogen carrier, although there is no obligation for the concerted movements of H^+ and e^- through the enzyme to follow parallel or identical pathways. Further tests of this proposed vectorial nitrate reductase could come from studies of inside-out vesicles, of the location of the reduced-Benzyl-Viologen-accepting site, and of the pH changes accompanying nitrate reduction by reduced Benzyl Viologen.

A study of the mechanism of proton-translocation associated with nitrate reductase may be particularly rewarding in view of the simplicity of the respiratory segment from ubiquinone to nitrate, which consists of only three (Enoch & Lester, 1974; MacGregor, 1975*a*) or possibly four (Clegg, 1975) polypeptides. In addition, this segment can be studied genetically (MacGregor, 1975*b*).

This work was supported by the Medical Research Council. J. A. D. was in receipt of a postgraduate studentship from the Science Research Council. The dual-wavelength spectrophotometer was constructed with the aid of a grant from The Royal Society. We acknowledge with pleasure the collaboration of Dr. Michael Kemp in the measurement of nitrate permeable spaces. Skilled technical assistance was provided by Mr. A. Tucker and Mr. D. Coutie.

References

Altendorf, K., Hirata, H. & Harold, F. M. (1975) *J. Biol. Chem.* **250**, 1405–1412
Beatrice, M. C. & Chappell, J. B. (1974) *Biochem. Soc. Trans.* **2**, 151–153
Brice, J., Law, J. F., Meyer, D. J. & Jones, C. W. (1974) *Biochem. Soc. Trans.* **2**, 523–526
Chappell, J. B. (1964) *Biochem. J.* **90**, 225–237
Clegg, R. A. (1975) *Biochem. Soc. Trans.* **3**, 691–693
Cohen, G. N. & Rickenberg, H. W. (1956) *Ann. Inst. Pasteur Paris* **91**, 693–720
Drozd, J. W. & Jones, C. W. (1974) *Biochem. Soc. Trans.* **2**, 529–531
Enoch, H. G. & Lester, R. L. (1972) *J. Bacteriol.* **110**, 1032–1040
Enoch, H. G. & Lester, R. L. (1974) *Biochem. Biophys. Res. Commun.* **61**, 1234–1241
Fick, A. (1855) *Philos. Mag. J. Sci. (London, Edinburgh and Dublin)* **10**, 30–39
Forget, P. (1974) *Eur. J. Biochem.* **42**, 325–332
Greville, G. D. (1969) *Curr. Top. Bioenerg.* **3**, 1–78
Griniuviene, B., Chmieliauskaite, V. & Grinius, L. (1974) *Biochem. Biophys. Res. Commun.* **56**, 1–8
Haddock, B. A. (1973) *Biochem. J.* **136**, 877–884
Harold, F. M. (1970) *Adv. Microb. Physiol.* **4**, 45–104
Heytler, P. G. (1963) *Biochemistry* **2**, 357–361
Hinkle, P. & Mitchell, P. (1970) *Bioenergetics* **1**, 45–60
Jeacocke, R. E., Niven, D. & Hamilton, W. A. (1972) *Biochem. J.* **127**, 57P
Jones, C. W., Brice, J. M., Downs, A. J. & Drozd, J. W. (1975) *Eur. J. Biochem.* **52**, 265–271
Kashket, E. R. & Wong, P. T. (1969) *Biochim. Biophys. Acta* **193**, 212–214
Kemp, M. B., Haddock, B. A. & Garland, P. B. (1975) *Biochem. J.* **148**, 329–333
Lawford, H. G. & Garland, P. B. (1972) *Biochem. J.* **130**, 1029–1044
Lawford, H. G. & Haddock, B. A. (1973) *Biochem. J.* **136**, 217–220
Lowry, O. H., Rosebrough, N. J., Farr, A. L. & Randall, R. J. (1951) *J. Biol. Chem.* **193**, 265–275
MacGregor, C. H. (1975*a*) *J. Bacteriol.* **121**, 1111–1116
MacGregor, C. H. (1975*b*) *J. Bacteriol.* **121**, 1117–1121
Meyer, D. J. & Jones, C. W. (1973) *Eur. J. Biochem.* **36**, 144–151
Mitchell, P. (1966) *Chemiosmotic Coupling in Oxidative and Photosynthetic Phosphorylation*, pp. 54–73, Glynn Research, Bodmin
Mitchell, P. & Moyle, J. (1967) *Biochem. J.* **104**, 588–600
Palmieri, F. & Klingenberg, M. (1967) *Eur. J. Biochem.* **1**, 439–446
Ruiz-Herrera, J., Showe, M. K. & De Moss, J. A. (1969) *J. Bacteriol.* **97**, 1291–1297
Scholes, P. & Mitchell, P. (1970) *Bioenergetics* **1**, 309–323
Sistrom, W. R. (1958) *Biochim. Biophys. Acta* **29**, 579–587
West, I. & Mitchell, P. (1972) *Bioenergetics* **3**, 445–462
White, S. H. & O'Brien, W. M. (1972) *Biochim. Biophys. Acta* **255**, 780–785
Wilson, A. C. & Pardee, A. B. (1962) *J. Gen. Microbiol.* **28**, 283–303